Published in final edited form as:
Plasma Process Polym. 2008 September 15; 5(7): 661–671. doi:10.1002/ppap.200700143.

Study of plasma modified-PTFE for biological applications: relationship between protein resistant properties, plasma treatment, surface composition and surface roughness

Nicolas Vandencasteele[1], **Bernard Nisol**[1], **Pascal Viville**[2], **Roberto Lazzaroni**[2], **David G. Castner**[3], and **François Reniers**[1,*]

[1]Université Libre de Bruxelles, Faculty of Sciences, Analytical and Interfacial Chemistry, cp 255, bld Triomphe 2, B-1050 Bruxelles, Belgium

[2]Laboratory for Chemistry of NoVel Materials, Université de Mons-Hainaut/Materia NoVa, Place du Parc, 20, B-7000 Mons, Belgium

[3]National ESCA and Surface Analysis Center for Biomedical Problems, Departments of Chemical Engineering and Bioengineering, University of Washington, Box 351750, Seattle, Washington 98195, USA

Abstract

PTFE samples were treated by low-pressure, O_2 RF plasmas. The adsorption of BSA was used as a probe for the protein resistant properties. The exposure of PTFE to an O_2 plasma leads to an increase in the chamber pressure. OES reveals the presence of CO, CO_2 and F in the gas phase, indicating a strong etching of the PTFE surface by the O_2 plasma. Furthermore, the high resolution C1s spectrum shows the appearance of CF_3, CF and C-CF components in addition to the CF_2 component, which is consistent with etching of the PTFE surface. WCA as high as 160° were observed, indicating a superhydrophobic behaviour. AFM Images of surfaces treated at high plasma power showed a increase in roughness. Lower amounts of BSA adsorption were detected on high power, O_2 plasma-modified PTFE samples compared to low power, oxygen plasma-modified ones.

Keywords

protein adsorption; biocompatibility; polytetrafluoroethylene (PTFE); plasma treatment; polymer modification

Introduction

Polytetrafluoroethylene (PTFE) is a hydrophobic material with interesting surface properties for biological applications.[1–12] The hydrophobic surface of the native polymer is due to the presence of a fully fluorinated backbone. The surface energy, as determined by contact angle measurements, can be modified by plasma treatment. Either the polar or the non polar

*Corresponding author: F. Reniers ; freniers@ulb.ac.be.

contribution of the surface energy can be tuned by this technique. The surface morphology, including the roughness, can be modified by the sputtering with the energetic ions generated in the plasma,[13–18] by etching due to active radicals or photons,[19–23] or by reticulation.[19] The surface composition can also be strongly modified by selective elimination (ie, "defluorination")[19] or by grafting of selected chemical functions, depending on the nature of the plasma gas.[24–28]

Many studies investigating the plasma surface modification of PTFE have already been published.[1, 11, 18, 19, 24–27, 29–38] Ryan & al.[19] observed that the oxygen plasma treatment of PTFE did not change the chemical composition of the surface, but it induced a roughening of the samples. Morra & al.[37] observed the same behavior for long plasma treatment times, but in their experiments they did observe some chemical change to the surface for the short treatment times (less than 5min.). For the longer treatment time there was a strong increase of the contact angle value due to the roughening of the surface. Liu & al.[18] also observed a strong etching of the surface with the oxygen RF plasma treatment, but in their case they observed some oxygen grafting onto the surface and a strong decrease of the contact angle values. Wilson & al. in [29]and [31] also observed an increase in the oxygen content and a decrease of the contact angle value for PTFE treated by a low-power oxygen plasma.

However, in many cases, the mechanism for surface modification remains mostly unknown. Moreover, there are few (no) data about the protein adsorption behavior of oxygen plasma – modified PTFE surfaces. The purpose of this paper is to perform carefully controlled plasma (oxygen) surface modification of PTFE, based on our previous studies,[39–41] followed by a compositional and morphological characterization of the surfaces. The modified surfaces are then exposed to protein solutions. From this strategy we expect to identify the key surface parameters responsible for protein adsorption onto plasma modified PTFE surfaces.

Protein adsorption onto surfaces is one of the key parameters for biocompatibility. Indeed, the first response of the body to the introduction of a foreign object is the adsorption of a layer of non-specific proteins onto it. The adsorbed proteins will then initiate a large number of biological reactions.[9] Our goal was to obtain surfaces where non-specific protein adsorption was minimized. Such surfaces can then be selectively modified by further processing to specifically adsorb selected proteins in well-defined conformations and orientations to enhance the biocompatibility of the surfaces.

Experimental

Polymer

Polytetrafluoroethylene was purchased from Goodfellow (1 mm thick sheet, Ref FP303050). After cutting to size, they were cleaned using pure ethanol (Normapur VWR) followed by pure isooctane (GR for analysis, Merck) before being introduced into the plasma chamber.

Plasma

The plasma chamber consisted of a stainless steel based vessel covered by a viton O-ring sealed Pyrex bell jar. The pumping system consisted of an Edwards primary pump

(pressures to 1.33 Pa) and a turbomolecular pump (Balzers 230 l/s) coupled to a membrane pump. Pure oxygen from Alphagaz was used (Alphagaz 2). Before introduction of oxygen, the chamber was pumped down to a pressure of 2.67 10^{-4} Pa and then backfilled to the working pressure. To avoid contamination, the chamber was continuously pumped during the experiments (dynamic regime). The flow rate of O_2 was set to 5 sccm. After treatment the chamber was backfilled to atmospheric pressure using pure nitrogen. The RF plasma was initiated using a Hüttinger PFG300RF generator operating at 13.56 MHz, coupled to a PFM1500A matching network. The electrode connected to the RF generator consist of an aluminium disc (diam. 42 mm) covered with a 0.8 mm thick borosilicate glass disc of the same diameter. The anode is made from a metallic grid. The distance between the anode and the cathode is 33 mm, the sample is placed 30 mm above the anode grid (Figure 1).

In this study, the results will be presented as a function of the plasma DC-Bias instead of RF power, as DC-Bias reflects better the electrical and energetic characteristics of the plasma than the injected power. The DC-Bias is measured at the RF cathode by means of high voltage probe connected directly to the RF generator. This Self-Bias comes from the difference in mobility between the electrons and ions in the plasma. Ions being heavier than electrons, they can not follow the RF electrical field, and therefore they remain mostly close to the cathode generating the DC-Bias[42]. We usually worked in the −600 V to −900 V DC-Bias range, which corresponds approximately to a power range of 20 W to 70 W in our geometry.

Since in a RF plasma the positive ions hit surfaces exposed to the glow with an energy depending on many parameters (pressure, electrode geometry ratio, power, etc.), the samples were positioned above the anode grid (grounded in the present study) outside the plasma region (afterglow mode). Above the grid electrode we expect that most of the plasma species interacting with the polymer surface will be neutrals (in this case, mostly atomic oxygen), as already shown in a previous study examining N_2 plasma – polyethylene interactions.[43]

Water Contact Angle

Water contact angle (WCA) measurements were performed on a Krüss DSA 100 instrument using ultra pure “Milli-Q” water (18 MΩ). The water droplets were deposited onto the surface by means of an automated syringe. Droplet volume was set to 3μL for the static drop measurement. For each sample 5 to 10 droplets were deposited onto different locations of the sample surface. The contact angle is automatically measured using the Drop Shape analysis software provided by Krüss and the Laplace-Young equation or the Tangent 1 method were used for calculating the angles. Results presented in this paper are the average of the angle measured on both sides of the drop (10–20 angles).

Dynamic measurements were done by increasing the volume of the drop from 2 μL to 15 μL at a rate of 30 μL/min, giving the advancing angle. Then the volume of the drop is decreased back to 2 μL at the same rate, giving the receding angle. The contact angle was measured every second during the advancing and receding processes.

X-ray photoelectron spectroscopy

X-ray photoelectron spectroscopy (XPS) analyses were performed on a Kratos AXIS Ultra DLD instrument equipped with a monochromatic Al Kα x-ray source. A photoelectron take off angle of 0° was used for all measurements. The photoelectron take-off angle is defined as the angle between the surface normal and the axis of the analyzer lens. The typical X-ray spot size was 700 × 300 μm^2. For each sample, the elemental composition was determined from survey scan and detailed N1s scans acquired using a pass energy of 80 eV. The N1s signal was used to quantify protein adsorption. High-resolution C1s spectra were acquired using a pass energy of 20 eV. All binding energies were referenced to the F1s peak at 689.7 eV. Three spots on each replicate were analysed and averaged to obtained the reported atomic percents (at. %). Data analysis was performed using CasaXPS (CasaSoftware Ltd.). The FWHM (at 20 eV pass energy) of the C1s peak from the clean PTFE sample was 1.5 eV. The C1s spectral envelope was fit with the lowest number of components physically meaningful (CF_3, CF_2, CF, C-CF, C-Ox and CC for the samples not exposed to the protein, with additional C-N, C-O, N-C=O components for the samples exposed to the protein).

Optical Emission spectroscopy

The plasma chamber is equipped with multiple (up to 8) fiber optic probes that were used to simultaneously detect the excited species generated by the plasma at the following locations: close to the cathode, middle of the plasma, close to the anode and close to the sample. The plasma was characterized using an Acton SpectralPro 2500i (Acton Research) optical emission spectrometer (OES) capable of a resolution of 0.06 nm and operating in the 200 nm – 900 nm region. The detector consisted in a Princeton Instrument Digital Camera type EEV with 400 × 1340 pixels. The spectra were recorded in the plasma and close to the sample.

Atomic Force Microscopy

All atomic force microscopy (AFM) images were recorded in ambient atmosphere at room temperature with a Nanoscope IIIa (Veeco, Santa Barbara, CA) microscope. The probes were commercially available silicon tips with spring constants of 24–52 N/m, resonance frequencies lying in the 264–339 kHz range, and a typical radius of curvature in the 10–15 nm range. The images were recorded with the highest available sampling resolution (512 × 512 pixels). The AFM microscope was operated in tapping mode to minimize the sample damage due to mechanical interactions between the AFM tip and the surface of the samples.

Protein adsorption

All protein adsorption experiments were done at room temperature. The protein used was bovine serum albumin (BSA) (Sigma, A-7638). Samples were cut to size and immersed in a phosphate buffer saline (PBS) solution for 20 minutes in a 24 well plate (Falcon Multiwell, VWR Scientific, PA), then the PBS solution was removed and the samples were immersed for 2h in a 0.1mg/mL protein/PBS solution. After adsorption, the samples were rinsed following the solution displacement protocol,[44] to avoid transferring protein from the air-water interface to the surface.

Results

PTFE treated by oxygen plasma

PTFE is a hydrophobic surface with a static WCA of 111.4°+/− 6.2° before isooctane cleaning and 103.6° +/− 8.8° after cleaning. Values reported in the literature range from 102.5°[15] to 130°.[20] Usually oxygen plasma treatment of polymers induce a decrease of the contact angle due to the grafting of new polar functionalities (-OH, =O, –OOH, etc.) onto the sample surface,[45–47] but in our experiments the oxygen plasma treatment of PTFE resulted in either a decrease or an increase of the contact angle, depending on the plasma power. Samples treated with a low power plasma were more hydrophilic than native PTFE. Those treated with a high power plasma were more hydrophobic. In this study samples with WCA as high as 160° could be obtained. Figure 2 presents the picture of a superhydrophobic PTFE surface obtained after 120 sec oxygen plasma at a working pressure of 6.66 Pa and a DC-BIAS of −936 V. Table 1 presents the evolution of the dynamic WCA as a function of the DC-Bias and the treatment time. For most highly hydrophobic surfaces (WCA >140°), the measurement of the contact angles becomes rather difficult, resulting in a strong increase of the standard deviation.

Table 1 also shows the surface elemental composition, as determined by XPS. We have to highlight that none of those samples contain nitrogen. This is important as we use the N1s signal, coming from the protein, to detect it's presence on the samples. Whereas no oxygen was detected on untreated PTFE, plasma treated PTFE surfaces contain up to 5 atomic percent oxygen at low or medium DC-Bias, but this concentration decreases at higher DC-bias until no oxygen is detected at −936 V DC-bias. The small sodium contamination detected on some oxygen plasma treated PTFE samples could come from the borosilicate glass placed at the cathode. The borosilicate glass could either be slightly sputtered or etched by HF formed during the plasma (H and F lines are detected in OES, hydrogen coming from the unavoidable residual water vapour). The peak fit high-resolution C1s spectra are dominated by components attributed to fluorinated species. Whereas new features corresponding to CF_3 (294 eV), CF (290 eV), C-CF or C-O_x (~287 eV) and CC appear, the major component remains CF_2 (Figure 3, left side). Some of the small increase in intensity in the 286 to 289 eV region could also be due to C-O_x species. This result is in agreement with some previous studies,[19],[21] but not with others.[18, 31] This difference could be explained by the difference of the plasma power used in the different experiments. Wilson & al.[31] used a 3 W power plasma, while in our studies we used power ranging from approximately 20 W to 70 W (corresponding to DC-Biases from −600 V to −900 V) and Ryan & al.[19] used a power of 20 W. In[19, 31, 39] unmonochromatized x-rays were used for the XPS analysis. In[19, 39] the C1s spectra showed no change except for the appearance of a small shoulder on the high binding energy side of the CF_2 peak and a slight broadening of this peak. The better energy resolution of the monochromatized x-ray source used in this study facilitates the identification of the different fluorocarbon components.

Surface morphology

The surface morphology was studied by AFM. Roughness values were determined over regions of 25, 110 and 225 μm^2. Figure 4 shows the evolution of the surface roughness

(RMS) and the WCA as a function of the DC-bias. Figure 5 presents some images of the pristine and plasma treated PTFE surfaces. At low plasma power (DC-bias of −250 V) a decrease of the RMS was observed, whereas at higher DC bias (−575 and −750 V) a strong increase of the RMS was observed. Before the plasma treatment the surface is relatively smooth and featureless, but after a high power oxygen plasma treatment an alveolar structure appears on the samples surfaces. The average size of the alveoles, as well as their depth, increases with DC-bias.

OES

The optical emission spectrum of a pure oxygen plasma shows 2 major lines, one at 777.4 nm[48] and another at 844.6 nm,[48] corresponding to transitions of atomic oxygen. During the O_2 plasma treatment of PTFE, the plasma color changes from yellow to blue. New emission lines corresponding to F (685,6[48] and 703,7 nm[49]),[50] CO bands (483.5 and 519.8 nm)[51] and CO_2^+ doublet at 289 nm[52] appear in the OES spectrum (Figure 6a and 6b). The identification of the emission lines is presented in Table 2 (the hydrogen line results probably from a small contamination by water vapour in the chamber). The appearance of these new lines, attesting for new gaseous species resulting from the interaction of atomic oxygen with the PTFE surface could explain the increase of the pressure that we had already observed.[41] It can be seen on figure 6 that small F signals are detected on the spectrum recorded without PTFE in the chamber. This comes from unavoidable previous contamination of the chamber which is used on a daily base to etch PTFE samples. Even after a mechanical cleaning and baking of the chamber (pressure after baking = 4×10^{-5} Pa) those small contamination remain present.

Characterization of samples after the protein adsorption

Surface composition—For all but the surfaces treated at the highest plasma power, between 3 and 5 atomic percent nitrogen was detected after BSA adsorption. Based on a previous study using XPS and ^{125}I radiolabeled to study BSA adsorption onto PTFE, this level of nitrogen signal corresponds to more than 250 ng/cm^2 of adsorbed protein.[53] The amount of nitrogen detected by XPS after BSA adsorption decreased to ~1 atomic percent at the highest plasma power used (Table 3), indicating this surface adsorbed less protein. This trend (high adsorption on untreated and low-power plasma treated PTFE surfaces low adsorption on high-power plasma treated PTFE surfaces) is confirmed by the analysis of the C1s spectral envelope. After BSA adsorption some new components from the protein (C-C, C-N, C-O, N-C=O)[53] appear, but these “protein” peaks are more pronounced for the low power plasma treated samples (Fig 2, right side). Finally, the concentrations of O increases and F decreases after BSA adsorption. This is a further proof for protein adsorption since oxygen is present in the BSA overlayer and the fluorine signal from the underlying substrate is attenuated by the adsorbed BSA.

Discussion

Oxygen plasma treatment of PTFE

The RF oxygen plasma treatment seems to mainly result in a chemical etching of the PTFE surface and not to an ion sputtering process. Indeed our samples are placed outside the

plasma, in the afterglow region, where there are much less energetic ions than inside the plasma. Furthermore our sample holder is placed at a floating potential (i.e. electrically insulated) , thus there is no important potential difference between the plasma and the sample. Moreover XPS results enable us to differentiate chemical etching from sputtering, the resulting shape of the C1s peak being significantly different. After sputtering the C1S peak of PTFE is broadened because of the damage done by the ions to the polymer chains, whereas after the chemical etching the C1s peak shape is mostly similar to the pristine one. Figure 7 shows a comparison of XPS C1s spectra between PTFE sample sputtered with oxygen ions and chemically etched with an oxygen plasma.This conclusion is also supported by the increase of the pressure in the plasma chamber during the treatment[40] and by previous studies from Morra & al.[37] and from our group.[39] The OES spectra also reveal the presence of CO, CO_2 and F lines in the oxygen plasma during the treatment of PTFE. As the samples were placed above the anode in the remote RF plasma region, the major reactive species reaching the surface would be oxygen atoms. The oxygen atoms would chemically etch the surface, in contrast to sputtering effects of O_2^+ or O^+ ions that are located close to the cathode. The shape of the C 1s peak is also consistent with chemical reaction of the PTFE surface by atomic oxygen, and not sputtering by ions, as we have shown previously.[39] Contrary to the O_2 plasma treatment of other polymers (PVDF, PE, PVF, etc.), the amount of oxygen functionalities grafted onto the PTFE surface remains very small (if any) and is dependent on the plasma power. For the low-power plasma treatments, or the very short (30s) high-power plasma treatment, only about 4 atomic % oxygen was grafted onto the PTFE surface. At the highest power plasma treatment no oxygen was detected.

After the high-power oxygen plasma treatment there is an increase of the WCA, with samples reaching values higher than 160° at high DC-bias. These surfaces can be considered to be super hydrophobic (defined as a surface with very high advancing and receding angles[54]). The high WCAs are mainly attributed to a change in the surface roughness. At low DC-bias, it seems that the plasma has a “cleaning” effect, removing surface impurities, and revealing the partly fibrous texture of the polymer (see Figure 5). This cleaning effect induces a decrease of the surface roughness, and a parallel decrease of the WCA, as shown in Figure 4. At higher DC-bias (and therefore, at higher energy), the AFM images show the presence of an alveolar structure. The chemical etching significantly increases the surface roughness of the samples. The alveolar structure could arise from the crystalline structure of the polymer, with the atomic oxygen preferentially etching the amorphous region of the sample compared to the crystalline region.[34, 55]

The increased surface roughness explains the super hydrophobic behavior of the high-power treated samples. The Wenzel and Cassie Baxter models relates the surface energy to the roughness of the sample. The equation for the Wenzel model[37] is:

$$\cos\theta = r\cos\theta' \quad (1)$$

where, θ is the Wenzel Angle, θ' is the Young Angle, r is the ratio between the effective and the geometric area.

In our case, however, the Cassie Baxter model seems to be more appropriate. The Cassie-Baxter model takes into account a two components surface, in our case PTFE and air trapped in the alveolar structure

The equation for the Cassie Baxter model[37] is:

$$cos\,\theta = F_1\,cos\,\theta_1 + F_2\,cos\,\theta_2 \quad (2)$$

where θ is the Cassie angle, the stable equilibrium contact angle of the liquid drop on the heterogeneous surface, θ_i and F_i are the Young angle and the fraction of surface relative to phase i, respectively. If the second component of the mixed interface is air trapped in the alveolar structure, equation (2) can be simplified.[56]

$$cos\,\theta = -1 + F_1\,(cos\,\theta_1 + 1) \quad (3)$$

where F_1 is the fraction of solid remaining in contact with the drop, $\theta_2 = 180°$ (the "contact angle" of a drop with air) and $F_2 = (1\text{-}F_1)$. Using $\theta_1 = 111.4°$ and $F_1 = 15\%$, equation (3) give us a contact angle of 154.8° which is in good agreement with our results. According to the Laplace equation and the alveolar size it is therefore very unlikely that water penetrates in the alveolar structure at atmospheric pressure.

By changing the plasma parameters (power, treatment time) the roughness and feature size of the PTFE surfaces can be systematically varied. The amount of oxygen grafted onto the surfaces can similarly be tuned between 0 and 5 atomic %. Low-power oxygen plasma treatment decreased in the surface roughness and contact angle (figure 4), resulting in a more hydrophilic surface. In contrast, high-power oxygen plasma treatment increased in the surface roughness and contact angle (figure 4), resulting in a more hydrophobic surface. Thus, PTFE can be made more hydrophilic or hydrophobic, which could explain the different results reported in the studies of Ryan & al.,[19] Morra & al.,[37] Liu & al.,[18] and Wilson & al.[29, 31] We also stress that, contrary to most other studies, our samples are placed outside the plasma discharge, in the afterglow region. We suggest the following tentative mechanism: the difference of behavior between high and low DC-Bias could come from the energy of the electrons in the plasma. At low energy electrons can't break the C-F bonds (5.3 eV) and the only reaction that can occur is the replacement of F atoms by the highly reactive oxygen radicals, this seems to be slow and inefficient. Once the electrons have enough energy (at high DC-Bias), they can possibly break C-F bonds, this leads to a all new set of possible reactions, chain breaking, and formation of CO_2.

Inside the plasma:

$$O_2 + e^- \rightarrow 2\,O^* + e^- \quad (1)$$

At the sample surface:

$$C - F + e^- \rightarrow C^* + F^* + e^- \quad (2)$$

$$C - C + e^- \rightarrow 2\,C^* + e^- \quad (3)$$

$$C^* + O^* \rightarrow CO \quad (4)$$

$$CO + O^* \rightarrow CO_2 \quad (5)$$

Protein adsorption

We have shown that XPS could detect the presence of adsorbed BSA through three observations: a) the appearance of the N 1s peak from the protein (no PTFE samples contain nitrogen before exposure to BSA); b) the decrease in the fluorine concentration (attenuation of the PTFE substrate by the adsorbed protein) and the increase in intensity in the oxygen concentration (BSA contains ca. 18 atomic % oxygen) and c) the appearance of protein related peaks (C-C, C-N, C-O, N-C=O) in the high resolution C 1s spectra. Our results suggest that PTFE samples treated in oxygen plasmas with moderate DC bias (−600 V), which result in some oxygen grafted onto the surface, have slightly highly amounts of adsorbed protein compared to untreated PTFE (i.e., ~5 atomic % nitrogen compared to ~3 atomic % nitrogen). In contrast, lower amounts of protein (1–2 atomic % nitrogen) are adsorbed onto PTFE samples treated with the highest power oxygen plasmas. The variation in the amount of adsorbed protein with the different surface treatment is probably not only due to the small changes in chemical composition of the treated surfaces, but also due to the changes in the physical structure of the samples. The ultra hydrophobic behavior minimizes the amount of protein adsorption observed on those samples. If we assume a two phase surface structure (Cassie-Baxter model) with air trapped in the alveolar structure, the trapped air could prevent the BSA solution from entering into the alveoles, thereby minimizing contact and adsorption of BSA onto the treated PTFE surface. Thus, different surfaces with similar chemical compositions but significantly different structures exhibit different protein adsorption behaviors.

Conclusion

We have modified PTFE surfaces by means of remote oxygen RF plasma treatments. We have shown that low-power and high-power plasma treatments create different surfaces. Low-power plasma treatment decreases the surface roughness and water contact angle, with a small amount of oxygen grafted onto the surface. In contrast, high-power plasma treatment produces superhydrophobic surfaces with significantly increased surface roughness. These results “reconcile” some of the previous results reported in the litterature. The results of our study show that both the chemical functionalities and physical structure of the surface are important for protein adsorption. Indeed, the adsorption of BSA onto treated PTFE can be minimized by increasing the surface roughness (i.e., superhydrophobic PTFE surfaces do not adsorb much BSA). Finally, this preliminary study shows that the chemical and structural tailoring of the PTFE surface by plasma treatment can control the amount of protein adsorbed onto those surfaces.

Acknowledgments

This research was supported by the FNRS (Belgium) (F. Reniers grant 2.4543.04) and by the Belgian Federal Government IAP – PAI "PSI – Fundamentals of plasma surface interactions"(P6-08) N. Vandencasteele wishes to thank the "Communauté Française de Belgique" for financial support allowing the collaboration with the NESAC/BIO. The surface analysis experiments at NESAC/BIO were supported by grant EB-002027 from the National Institutes of Health (USA). Chi-Ying Lee, Lara Gamble and Roger Michel are thanked for technical assistance with protein adsorption and XPS experiments.

References

[1]. Baquey C, Palumbo F, Porte-Durrieu MC, Legeay G, Tressaud A, d'Agostino R. Nuclear Instruments and Methods in Physics Research Section B: Beam Interactions with Materials and Atoms. 1999; 151:255.

[2]. Grainger DW, Pavon-Djavid G, Migonney V, Josefowicz M. Journal of Biomaterials Science-Polymer Edition. 2003; 14:973. [PubMed: 14661874]

[3]. Gudipati CS, Greenlief CM, Johnson JA, Prayongpan P, Wooley KL. Journal of Polymer Science Part a-Polymer Chemistry. 2004; 42:6193.

[4]. Puskas JE, Chen YH. Biomacromolecules. 2004; 5:1141. [PubMed: 15244424]

[5]. Rasmusson JR, Erlandsson R, Salaneck WR, Schott M, Clark DT, Lundstrom I. Scanning Microscopy. 1994; 8:481.

[6]. Singh S, Baker JL. Clinics in Plastic Surgery. 2000; 27:579. [PubMed: 11039891]

[7]. Wang P, Tan KL, Kang ET. Journal of Biomaterials Science-Polymer Edition. 2000; 11:169. [PubMed: 10718477]

[8]. Zardeneta G, Mukai H, Marker V, Milam SB. Journal of Oral and Maxillofacial Surgery. 1996; 54:873. [PubMed: 8676233]

[9]. Castner DG, Ratner BD. Surface Science. 2002; 500:28.

[10]. Makohliso SA, Giovangrandi L, Leonard D, Mathieu HJ, Ilegems M, Aebischer P. Biosensors and Bioelectronics. 1998; 13:1227. [PubMed: 9871978]

[11]. Markkula TK, Hunt JA, Pu FR, Williams RL. Surface and interface analysis. 2002; 34:583.

[12]. Favia, P.; Milella, A.; Iacobelli, L.; d'Agostino, R. Plasma pre-treatment and treatments on polytetrafluorethylene for reducing the hydrophobic recovery. In: d'Agostino, R.; Favia, P.; Wertheimer, MR.; Oehr, C., editors. Plasma Processes and Polymers. Wiley - VCH; 2005.

[13]. Zhang J, Yu X, Li H, Liu X. Applied Surface Science. 2002; 185:255.

[14]. Colwell JM, Wentrup-Byrne E, Bell JM, Wielunski LS. Surface and Coatings Technology. 2003; 168:216.

[15]. Inoue Y, Yoshimura Y, Ikeda Y, Kohno A. Colloids and Surfaces B: Biointerfaces. 2000; 19:257.

[16]. Zhang J, Xu L, Yu X, Liu X. Materials Letters. 2002; 56:410.

[17]. Inagaki N, Tasaka S, Umehara T. Journal of Applied Polymer Science. 1999; 71:2191.

[18]. Liu CZ, Wu JQ, Ren LQ, Tong J, Li JQ, Cui N, Brown NMD, Meenan BJ. Materials Chemistry and Physics. 2004; 85:340.

[19]. Ryan ME, Badyal JPS. Macromolecules. 1995; 28:1377.

[20]. Niino H, Yabe A. Applied Surface Science. 1996; 96–98:550.

[21]. Dalins I, Karimi M. Journal of Vacuum Science & Technology a-Vacuum Surfaces and Films. 1992; 10:2921.

[22]. Grossman E, Gouzman I. Nuclear Instruments & Methods in Physics Research Section B-Beam Interactions with Materials and Atoms. 2003; 208:48.

[23]. Girardeaux C, Idrissi Y, Pireaux JJ, Caudano R. Applied Surface Science. 1996; 96–98:586.

[24]. Caro JC, Lappan U, Simon F, Pleul D, Lunkwitz K. European Polymer Journal. 1999; 35:1149.

[25]. Chevallier P, Castonguay N, Turgeon S, Dubrulle N, Mantovani D, McBreen PH, Wittmann JC, Laroche G. Journal of Physical Chemistry B. 2001; 105:12490.

[26]. Yamada Y, Yamada T, Tasaka S, Inagaki N. Macromolecules. 1996; 29:4331.

[27]. Konig U, Nitschke M, Pilz M, Simon F, Arnhold C, Werner C. Colloids and Surfaces B-Biointerfaces. 2002; 25:313.

[28]. Xu H, Hu Z, Wu S, Chen Y. Material chemistry and physics. 2002; 9710:1.

[29]. Wilson DJ, Eccles AJ, Steele TA, Williams RL, Pond RC. Surface and interface analysis. 2000; 30:36.

[30]. Pringle SD, Joss VS, Jones C. Surface and interface analysis. 1996; 24:821.

[31]. Wilson DJ, Williams RL, Pond RC. Surface and interface analysis. 2001; 31:385.

[32]. Chen JR, Wakida T. Journal of Applied Polymer Science. 1997; 63:1733.

[33]. Kim SR. Journal of Applied Polymer Science. 2000; 77:1913.

[34]. Youngblood JP, McCarthy TJ. Macromolecules. 1999; 32:6800.

[35]. Tan KL, Woon LL, Wong HK, Kang ET, Neoh KG. Macromolecules. 1993; 26:2832.

[36]. Yu QS, Reddy CM, Meives MF, Yasuda HK. Journal of Polymer Science Part a-Polymer Chemistry. 1999; 37:4432.

[37]. Morra M, Occhiello E, Garbassi F. Langmuir. 1989; 5:872.

[38]. Badey JP, Espuche E, Sage D, Chabert B. Polymer. 1996; 37:1377.

[39]. Vandencasteele N, Fairbrother H, Reniers F. Plasma Processes and Polymers. 2005; 2:493.

[40]. Vandencasteele N, Reniers F. Surface and Interface Analysis. 2004; 36:1027.

[41]. Vandencasteele N, Merche D, Reniers F. surface and interface analysis. 2006; 38:526.

[42]. Chapman, B., editor. Glow Discharge Processes Sputtering and plasma etching. John Wiley & Sons; New York: 1980.

[43]. Wagner AJ, Fairbrother DH, Reniers F. Plasmas and polymers. 2003; 8:119.

[44]. Techniques in Biocompatibility Testing. Vol. Vol. 2. Williams; Boca Raton, FL: 1986.

[45]. Aumann T, Theirich D, Engemann J. Surface and Coatings Technology. 2001; 142–144:169.

[46]. Park YW, Inagaki N. Polymer. 2003; 44:1569.

[47]. Shahidzadeh-Ahmadi N, Chehimi MM, Arefi-Khonsari F, Foulon-Belkacemi N, Amouroux J, Delamar M. Colloids and Surfaces A: Physicochemical and Engineering Aspects. 1995; 105:277.

[48]. Watanabe N, Buscher W, Bohm G. Analytical Sciences. 2001; 17:i971.

[49]. Kim D-P, Kim C-I. Thin Solid Films. 2003; 434:130.

[50]. Ralchenko, Y.; Kramida, AE.; Reader, J. NIST. 2007.

[51]. Goujon M, Belmonte T, Henrion G. Surface and Coatings Technology. 2004; 188–189:756.

[52]. Farley DR, Cattolica RJ. Journal of Quantitative Spectroscopy and Radiative Transfer. 1996; 56:83.

[53]. Tidwell CD, Castner DG, Golledge SL, Ratner BD, Meyer K, Hagenhoff B, Benninghoven A. Surface and Interface Analysis. 2001; 31:724.

[54]. Chen W, Fadeev AY, Hsieh MC, Oner D, Youngblood J, McCarthy TJ. Langmuir. 1999; 15:3395.

[55]. Fresnais J, Benyahia L, Chapel JP, Poncin-Epaillard F. European Physical Journal-Applied Physics. 2004; 26:209.

[56]. Quere D. Physica a-Statistical Mechanics and Its Applications. 2002; 313:32.

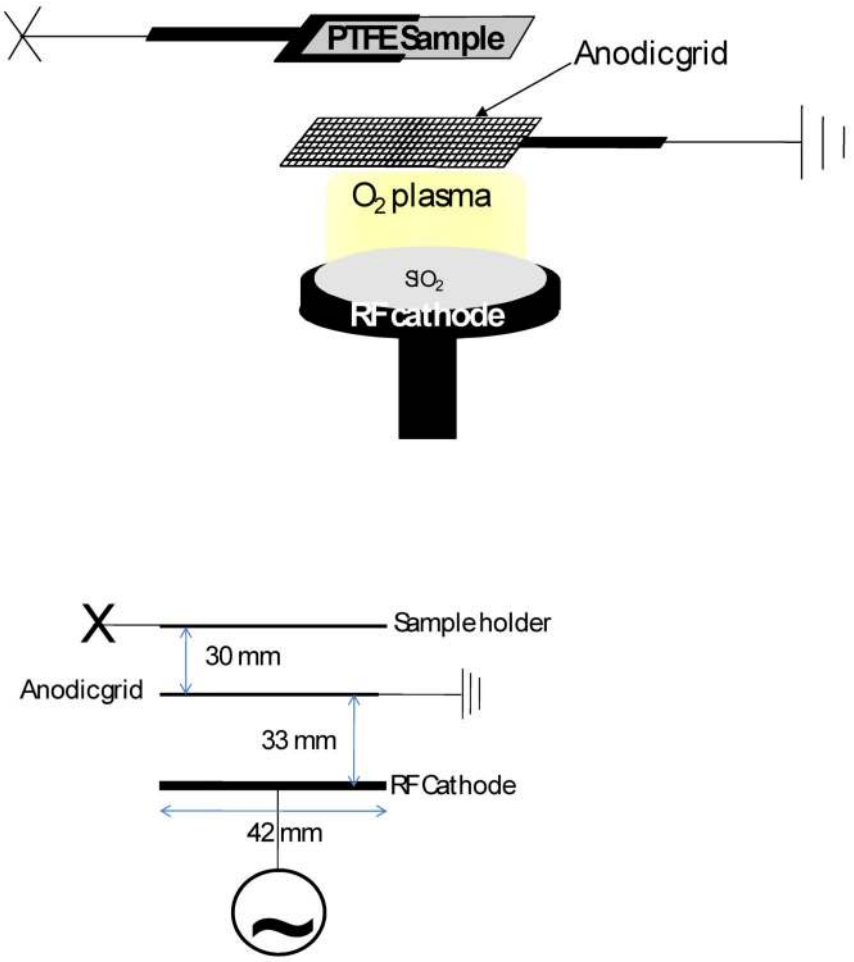

Figure 1.
Schematic of the electrode and sample geometry.

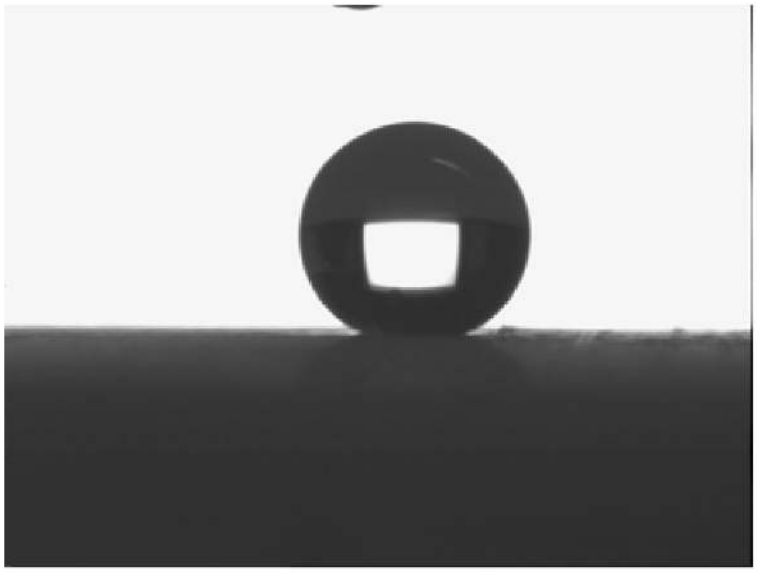

Figure 2.

Droplet of ultra pure water (V = 3 μL) deposited onto a oxygen plasma treated PTFE surface. Plasma treatment conditions were p = 6.66 Pa, DC-BIAS = −936 V, t = 120 sec. The water contact angle was >160°.

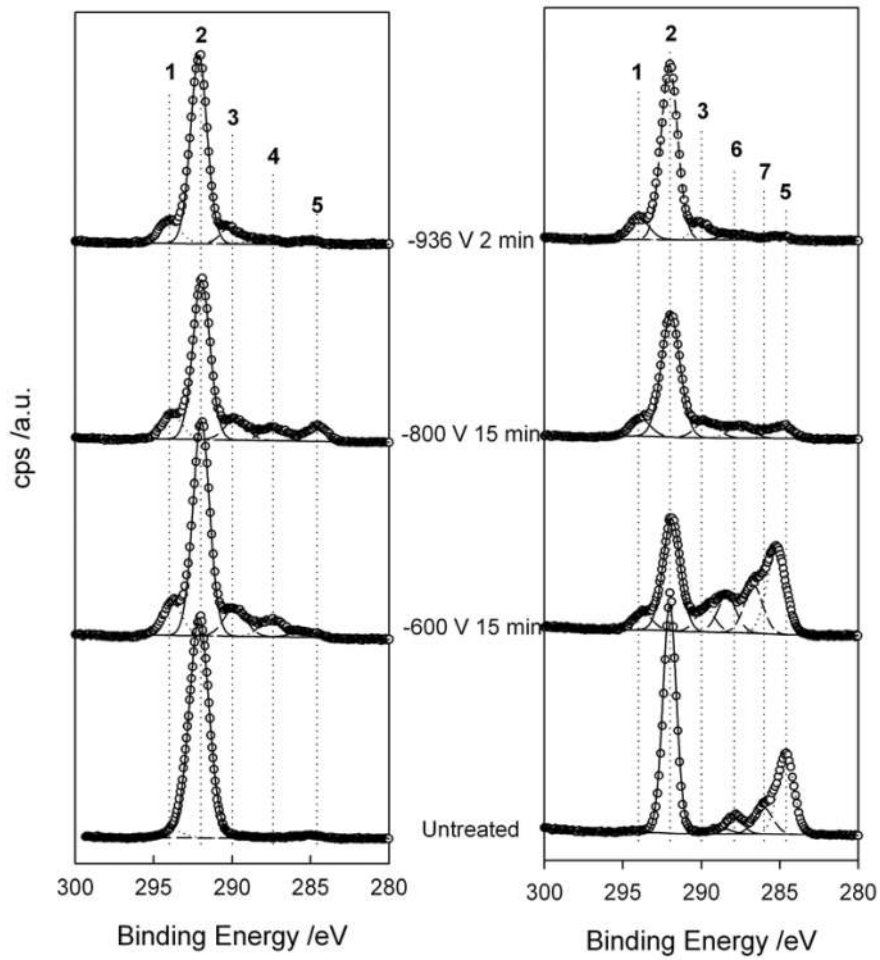

Figure 3.

Comparison of the high resolution C1s spectra of oxygen plasma treated PTFE before (left) and after (right) BSA exposure for different plasma powers (p = 6.66 Pa). The peak assignments are: **1** CF_3 (294 eV), **2** CF_2 (292 eV), **3** CF (290 eV), **4** C-CF and/or C-O_x (287.4 eV), **5** CC (284.6 eV), **6** N-C=O (288.2 eV) and **7** C-O and/or C-N (286 eV).

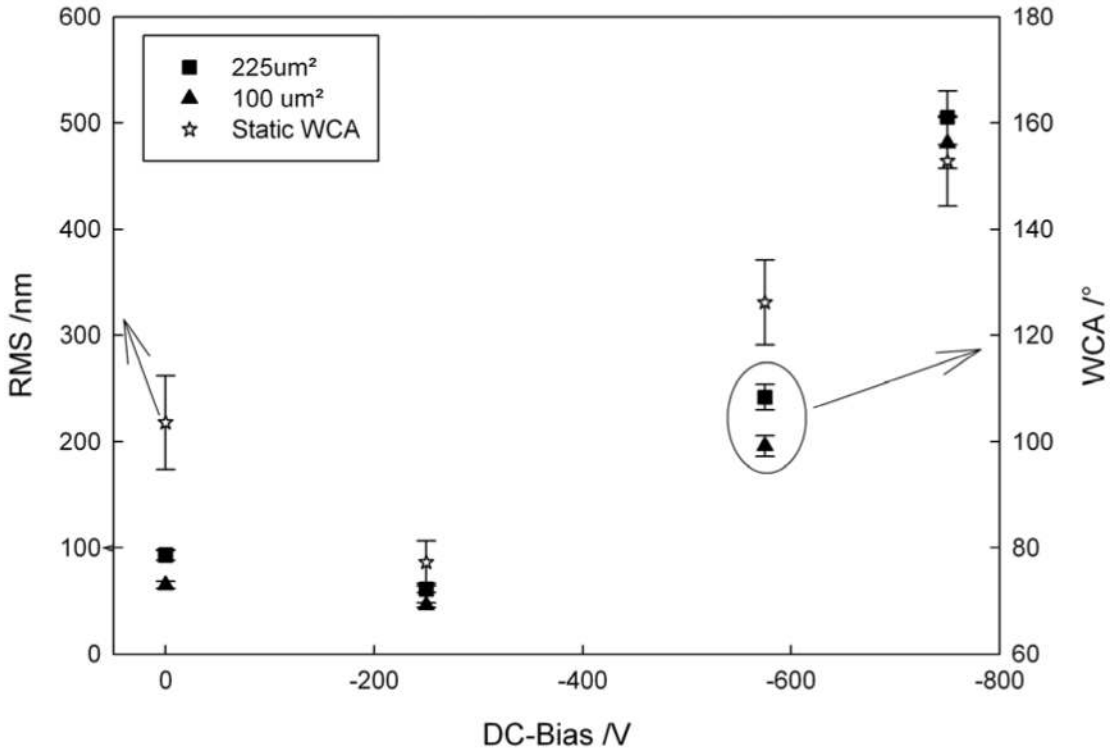

Figure 4.

Root mean squared surface roughness coefficient (triangle and square, left X axis) and water contact angle (star, right X axis) as a function of DC-BIAS for PTFE treated in an oxygen plasma at 6.66 Pa for 700s.

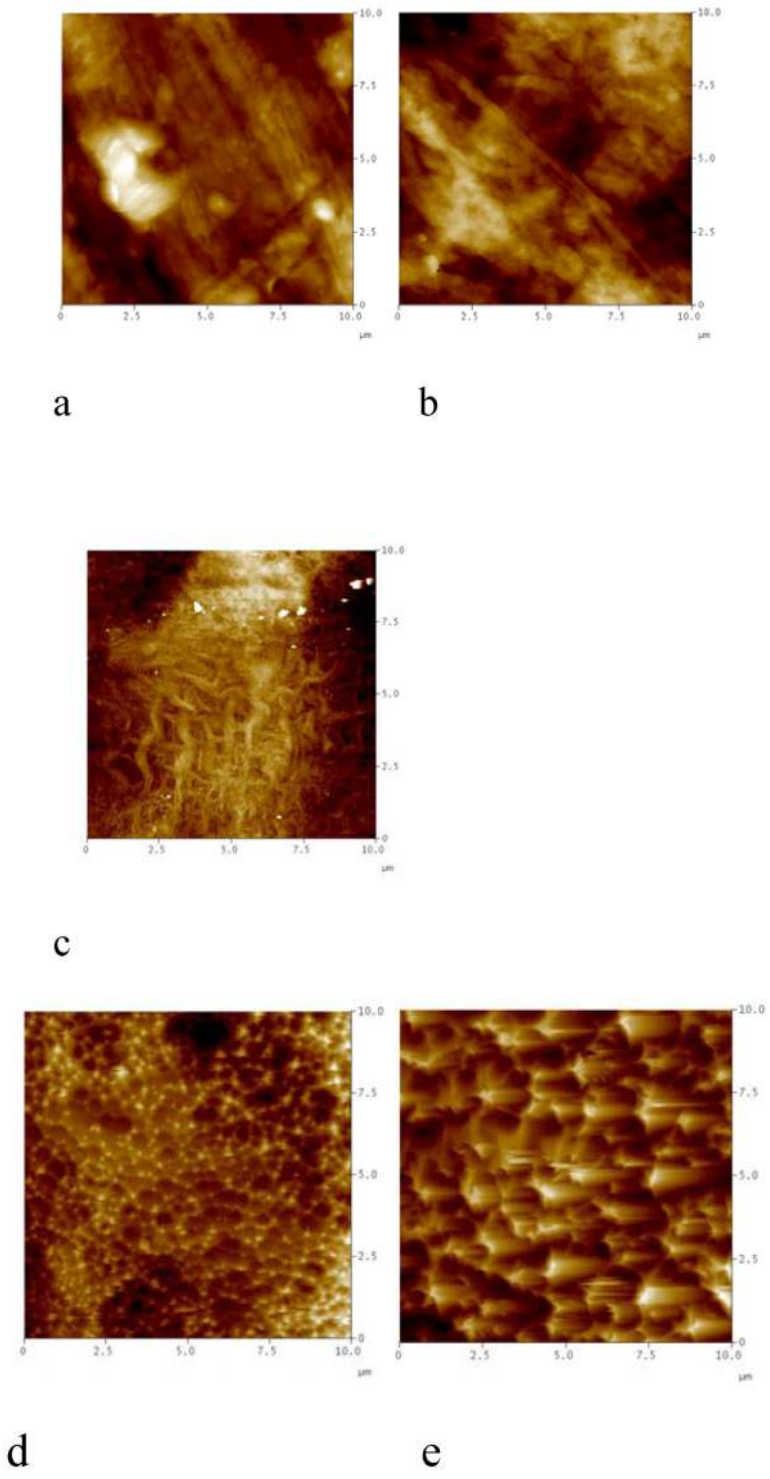

Figure 5.

AFM images of a) as received PTFE; b) PTFE washed with isooctane; c) PTFE treated with a −250 V DC-bias oxygen plasma; d) PTFE treated with a −575 V DC-bias oxygen plasma; e) PTFE treated with a −750 V DC-bias oxygen plasma. The measured surface roughnesses of these surfaces are shown in Figure 3.

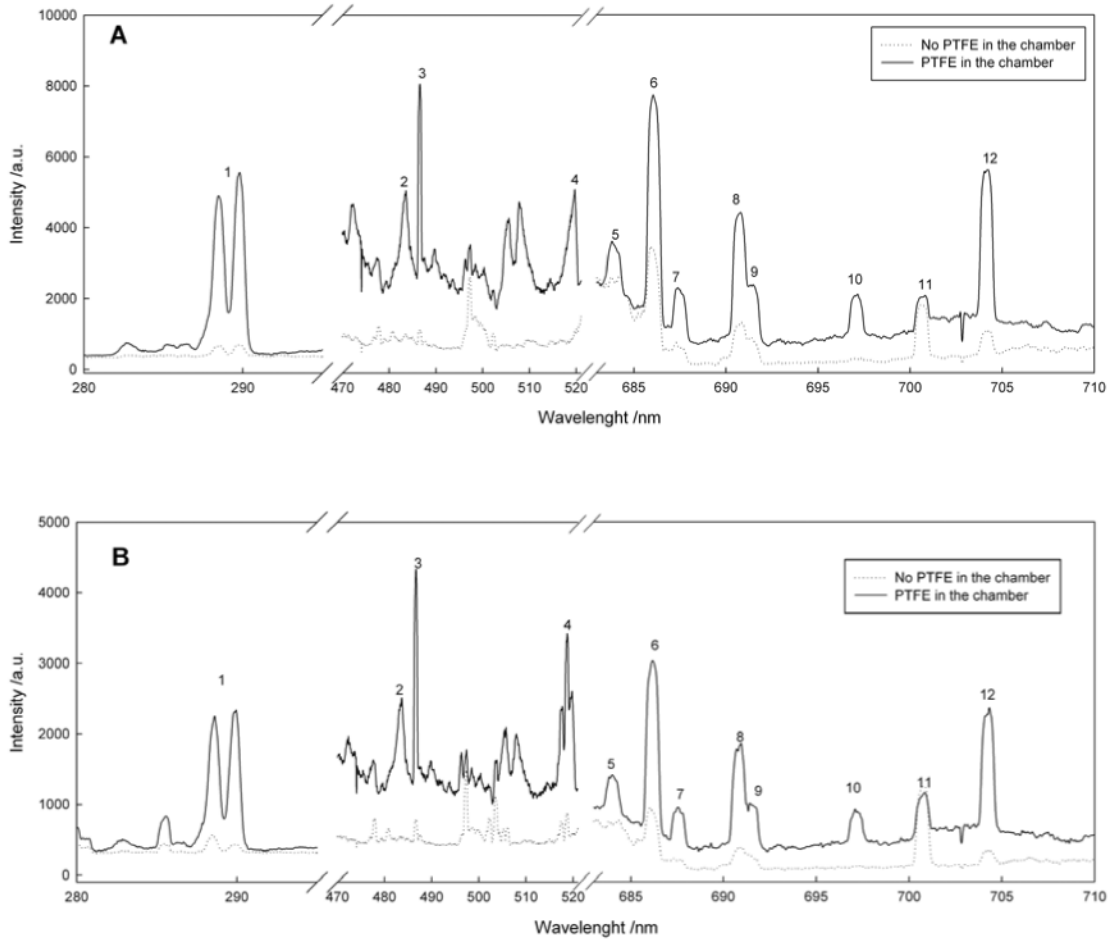

Figure 6.

Optical emission spectra of the oxygen plasma without (dotted line) and with (solid line) a PTFE sample in the chamber. The DC-BIAS was −1000V and p(O_2) was 6.66 Pa. Spectra A were recorded in the plasma phase, spectra B were recorded close to the sample.

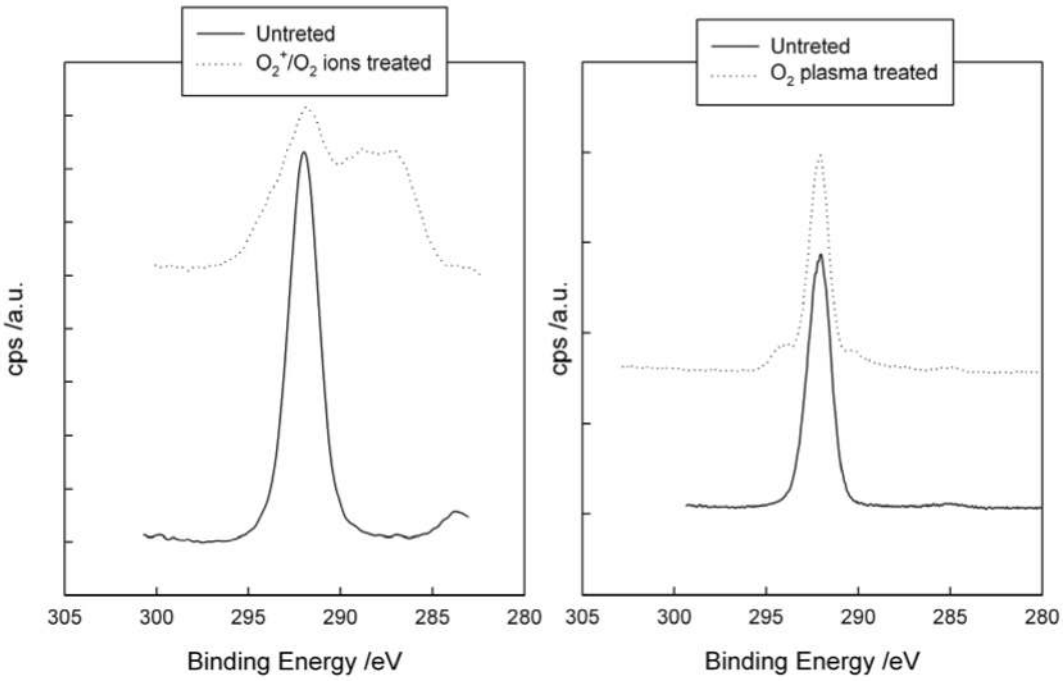

Figure 7.

Comparison between HRC1s peak for PTFE sputtered with oxygen (left) or chemically etched by an oxygen plasma (right). Sputtering parameters: gas = O_2, E = 4 kV, I = 10 mA, P(in the ion gun) = 10 mPa, sputter time = 60 min. Chemical etching parameter: gas = O_2, DC-Bias = −936 V, p = 6.66 Pa, etching time = 2 min

Table 1

Elemental compositions, determined by XPS and dynamic water contact angles of PTFE before and after oxygen plasma treatment (variable power and treatment time, p = 6.66 Pa). Standard deviations are approximately 1 at.% for fluorine and carbon and approximately 0.3 at.% for oxygen. nd = not detected. For the two last lines, no dynamic contact angle could be measured as the samples being too hydrophobic.

Advancing Angle /°	Receding Angle /°	DC-BIAS	Time /s	Atomic % fluorine	Atomic % oxygen	Atomic % carbon	Atomic % nitrogen	Atomic % sodium
118.3	114.7	0V	0	66.7	nd	33.3	0	0
120.9	85.7	−600V	30	49.8	4.5	45.7	0	0
121.8	104.7	−600V	300	52.1	4.7	42.9	0	0.3
143.3	131.7	−600V	900	52.7	2.9	44.4	0	0
127.4	103.9	−800V	30	50	3.9	46.1	0	0
156.7	146.4	−800V	300	51.2	2.7	44.7	0	1.4
-	-	−800V	900	53.9	2.1	43.2	0	0.8
-	-	−936V	120	57	nd	41.8	0	1.2

Table 2

Assignment of the optical emission lines observed in Figure 5.

		Wavelength /nm	Transition	Terms	$J_i - J_k$	Ref
1	CO_2^+	289.0	$B^2\Sigma_u^+ \rightarrow X^2\Pi_g$			[52]
2	CO	483.5	$B^1\Sigma \rightarrow A^1\Pi$ (ν ;ν') (0,1)			[51]
3	H	486.1	4d → 2p	$^2D \rightarrow {}^2P^\circ$	5/2 – 3/2	[50]
4	CO	519.8	$B^1\Sigma \rightarrow A^1\Pi$ (ν ;ν') (0,2)			[51]
5	F	683.4	$2s^22p^4(^3P)3p \rightarrow 2s^22p^4(^3P)3s$	$^4D^\circ \rightarrow {}^4P$	3/2 – 3/2	[50]
6	F	685.6	$2s^22p^4(^3P)3p \rightarrow 2s^22p^4(^3P)3s$	$^4D^\circ \rightarrow {}^4P$	7/2 – 5/2	[50]
7	F	687.0	$2s^22p^4(^3P)3p \rightarrow 2s^22p^4(^3P)3s$	$^4D^\circ \rightarrow {}^4P$	½ – ½	[50]
8	F	690.2	$2s^22p^4(^3P)3p \rightarrow 2s^22p^4(^3P)3s$	$^4D^\circ \rightarrow {}^4P$	5/2 – 3/2	[50]
9	F	691.0	$2s^22p^4(^3P)3p \rightarrow 2s^22p^4(^3P)3s$	$^4D^\circ \rightarrow {}^4P$	3/2 – ½	[50]
10	F	696.6	$2s^22p^4(^3P)3p \rightarrow 2s^22p^4(^3P)3s$	$^2P^\circ \rightarrow {}^2P$	½ – 3/2	[50]
11	O	700.2	$2s^22p^3(^4S^\circ)4d \rightarrow 2s^22p^3(^4S^\circ)3p$	$^3D^\circ \rightarrow {}^3P$	3 – 2	[50]
12	F	703.7	$2s^22p^4(^3P)3p \rightarrow 2s^22p^4(^3P)3s$	$^2P^\circ \rightarrow {}^2P$	3/2 – 3/2	[50]

Table 3

XPS determined elemental compositions of the PTFE samples after exposure to BSA.

DC-BIAS /V	Time /s	F 1s	O 1s	C 1s	N 1s
0	0	39.8 +/– 1.4	4.1 +/– 0.3	53.1 +/– 1.2	3.0 +/– 0.3
–600	30	36.2 +/– 5.8	7.8 +/– 0.3	51.7 +/– 5.2	4.2 +/– 0.4
–600	300	29.1 +/– 1.3	9.0 +/– 0.4	56.6 +/– 1.7	5.2 +/– 0.1
–600	900	31.1 +/– 0.6	7.7 +/– 0.1	56.6 +/– 0.6	4.6 +/– 0.2
–800	30	31.9 +/– 1.7	6.8 +/– 0.8	56.9 +/– 0.8	4.4 +/– 0.3
–800	300	33.6 +/– 0.6	7.0 +/– 0.4	55.3 +/– 0.8	4.1 +/– 0.1
–800	900	48.1 +/– 4.7	4.3 +/– 1.9	45.6 +/– 2.9	2.1 +/– 1.4
–936	120	51.6 +/– 5.2	2.6 +/– 2.1	44.4 +/– 1.9	1.3 +/– 1.7